A Novel Label-Free Approach for Post-Fire Environmental Assessment Based on Zero-Shot Segment Anything Model (SAM)

Melih ALTAY[1], Fatih Fehmi SIMSEK[2], Saygin ABDIKAN[3]

[1] Department of Geomatics Engineering, Hacettepe University, Ankara 06800, Türkiye – melihaltay17@hacettepe.edu.tr
[2] TÜBİTAK Space Technologies Research Institute, Ankara 06800, Türkiye – fehmi.simsek@tubitak.gov.tr
[3] Department of Geomatics Engineering, Hacettepe University, Ankara 06800, Türkiye – sayginabdikan@hacettepe.edu.tr

Keywords: Burned Area Mapping, Deep Learning, Segment Anything Model (SAM), Sentinel-2, Zero-Shot Segmentation

Abstract

Accurate and timely burned-area delineation is essential for quantifying wildfire impacts on ecosystem functioning, carbon dynamics, and post-fire recovery. Conventional pixel-based approaches remain sensitive to spectral ambiguity, topographic effects, and empirically defined thresholds, while recent deep learning models (e.g., U-Net, DeepLab, SegFormer) are constrained by their dependence on large, site-specific labelled datasets and repeated regional retraining. This study proposes a zero-shot burned-area mapping framework based on the Segment Anything Model (SAM) and multispectral Sentinel-2 imagery. Composite representations derived from ΔNBR, ΔNBR2, and ΔNDVI were generated and used as primary inputs to SAM in a label-free configuration. The effects of alternative pre-processing strategies, post-processing operations, and key hyperparameter settings were systematically investigated. Results show that multi-scale inference (crop_n_layers = 2) substantially improves geometric consistency and boundary accuracy of the extracted burned-area masks. The highest Intersection over Union values reached 0.89 for the Bursa study site and 0.87 for the Çanakkale study site, with corresponding F1 scores of 0.94 and 0.92, respectively. Despite the complete absence of training samples, SAM achieves performance comparable to, and in some cases exceeding, that of supervised deep learning approaches. Furthermore, integrating index-based composites with SAM outputs significantly enhances the discrimination between burned and unburned surfaces by reducing boundary fragmentation and spectral confusion in heterogeneous landscapes. By eliminating the need for manually labeled training data, the proposed framework addresses a major operational bottleneck in deep learning–based remote sensing. Overall, the study demonstrates a fast, scalable, and cost-effective solution for operational burned-area mapping and highlights the strong potential of SAM for zero-shot environmental monitoring and rapid post-fire response.

1. INTRODUCTION

Rapid and reliable burned-area mapping constitutes a fundamental prerequisite for post-fire environmental assessment, operational response planning, and long-term ecosystem management. Forest fires represent one of the most influential natural disturbance agents in terrestrial ecosystems, generating complex and multidimensional impacts on the carbon cycle, biodiversity, hydrological processes, and land-cover dynamics (Bowman et al., 2009; Keeley et al., 2012). Fire-induced vegetation loss and soil alteration significantly modify surface energy balance, greenhouse gas emissions, and landscape connectivity, while simultaneously shaping ecosystem resilience and recovery trajectories (Bond and Keeley, 2005; van der Werf et al., 2017). These impacts are particularly pronounced in Mediterranean-type environments, where prolonged drought conditions, rising temperatures, and increasing anthropogenic pressure have contributed to a marked escalation in both fire frequency and severity in recent decades (Pausas and Fernández-Muñoz, 2012; Turco et al., 2018). Under such rapidly evolving environmental conditions, the timely production of reliable burned-area maps has become an essential component of ecosystem restoration planning, fire management strategies, and decision-support systems.

Satellite remote sensing has emerged as the principal data source for burned-area monitoring due to its capability to provide consistent, multi-temporal, and synoptic observations over large geographic extents (Chuvieco et al., 2019; Roy et al., 2008). In operational practice, burned-area detection has traditionally relied on spectral index–based approaches, particularly the Normalized Difference Vegetation Index (NDVI) (Rouse et al., 1974) and the Normalized Burn Ratio (NBR), including its derivative forms such as differenced NBR (dNBR) and NBR2 (Key and Benson, 2006). These indices are widely adopted because of their conceptual simplicity, computational efficiency, and integration into standardized fire impact assessment frameworks. However, despite their extensive use, index-based approaches remain highly sensitive to vegetation heterogeneity, illumination variability, atmospheric disturbances, and acquisition geometry (Lentile et al., 2006). Spectral similarities between burned surfaces, bare soil, dark lithological units, moist soils, and water bodies frequently generate classification ambiguity, while topographic effects introduce additional radiometric inconsistencies. Consequently, the determination of globally transferable threshold values remains problematic, and the robustness of purely index-driven classification approaches often deteriorates across different ecosystems, terrain configurations, and sensor characteristics (Chuvieco et al., 2006). Although radiometric correction and topographic normalization techniques have been proposed to mitigate these limitations, such preprocessing pipelines increase operational complexity and do not consistently guarantee stable cross-regional performance.

To address these shortcomings, deep learning–based semantic segmentation approaches have gained substantial attention in burned-area mapping over the past decade. Convolutional neural network (CNN) architectures such as U-Net (Ronneberger et al., 2015), Fully Convolutional Networks (FCN) (Long et al., 2015), and DeepLabV3+ (Chen et al., 2018) have demonstrated notable improvements in spatial coherence and boundary delineation compared with conventional machine-learning and threshold-based techniques. By learning hierarchical and context-aware feature representations, these models effectively discriminate burned and unburned surfaces even in spectrally complex environments and have been successfully applied to multispectral satellite imagery (Zhu et al., 2017). Recent studies have further incorporated vegetation indices, multi-temporal image stacks, and multi-sensor data including optical and synthetic aperture radar (SAR) observations to reduce spectral ambiguity and enhance classification robustness (Belenguer-Plomer et al., 2021). Despite these advances, the operational scalability of deep learning frameworks remains constrained by their reliance on large volumes of high-quality labeled data.

Ground-truth generation typically requires intensive manual annotation, field validation, and region-specific quality assurance procedures. Moreover, trained models often exhibit performance degradation when transferred to new geographic regions, distinct land-cover compositions, or alternative sensor characteristics, thereby necessitating repeated retraining and domain-specific optimization.

Recent progress in computer vision has introduced a new methodological paradigm based on large-scale foundation models trained on extensive and diverse datasets, enabling adaptation to downstream tasks through prompt-based interaction mechanisms. Within this context, the Segment Anything Model (SAM) has attracted considerable attention due to its capacity to generate high-quality segmentation masks in a zero-shot setting without task-specific fine-tuning (Kirillov et al., 2023). Trained on more than one billion masks, SAM offers a promising opportunity to mitigate the long-standing dependence on labeled datasets that restricts the practical deployment of supervised deep learning models in remote sensing applications. Nevertheless, despite its rapid adoption in general computer vision tasks, the application of SAM to burned-area detection remains limited and largely exploratory. The direct transfer of a generic vision foundation model to multispectral satellite imagery raises critical questions concerning spectral representation, preprocessing design, and the reliability of zero-shot segmentation under complex land-surface conditions.

In this study, we introduce a spectrally guided zero-shot burned-area mapping framework that leverages the generalization capability of SAM while explicitly incorporating multi-temporal spectral change information derived from Sentinel-2 imagery (Drusch et al., 2012). Rather than applying SAM to conventional true-color composites, change-sensitive spectral indices including ΔNBR, ΔNBR2, and ΔNDVI are integrated into an RGB-like composite representation designed to guide the model’s mask generation mechanism toward fire-affected regions. By embedding physically meaningful spectral responses into the SAM input space, the proposed framework aims to bridge the gap between generic vision-based segmentation and domain-specific burned-area characterization.

The primary objective of this research is to systematically evaluate the zero-shot performance of SAM for automated burned-area detection using multispectral Sentinel-2 data and to assess whether segmentation accuracy comparable to supervised deep learning architectures can be achieved without any labeled training samples. Within this scope, the study investigates: (i) the influence of different preprocessing and post-processing strategies under conditions characterized by land-cover heterogeneity, complex terrain, and persistent spectral ambiguity; (ii) the impact of key SAM configuration parameters including points_per_side, crop_n_layers, pred_iou_thresh, and stability_score_thresh on segmentation accuracy, geometric consistency, and boundary delineation; and (iii) the overall applicability, strengths, and limitations of foundation-model-based segmentation for post-fire mapping through comprehensive quantitative evaluation using Precision, Recall, Intersection over Union (IoU), and F1-score metrics, complemented by qualitative visual analysis.

By presenting one of the first systematic assessments of SAM for burned forest area detection, this study proposes a label-free, computationally efficient, and operationally flexible alternative to conventional supervised deep learning workflows. The framework directly addresses persistent challenges related to manual annotation requirements, limited regional transferability, and constrained model generalization. More broadly, the findings highlight the strategic potential of zero-shot foundation models as scalable and cost-effective solutions for environmental monitoring, offering a promising pathway for integrating large-scale pre-trained segmentation models into operational remote sensing workflows and future global fire monitoring systems.

2. METHODOLOGY AND ZERO-SHOT SAM FRAMEWORK

2.1 Data Acquisition and Pre-processing

The proposed framework was evaluated using two complex and heterogeneous wildfire events in Türkiye, namely the 2020 fire in the Bursa region (sub-divided into Bursa-a and Bursa-b for detailed analysis) and the 2023 fire in the Çanakkale region (Figure 1). These two study areas were deliberately selected due to their contrasting land-cover compositions, rugged topographic characteristics, and the presence of spectrally heterogeneous surfaces such as mixed forest stands, agricultural fields, bare soil, and rocky terrain, which pose significant challenges for conventional burned-area mapping approaches.

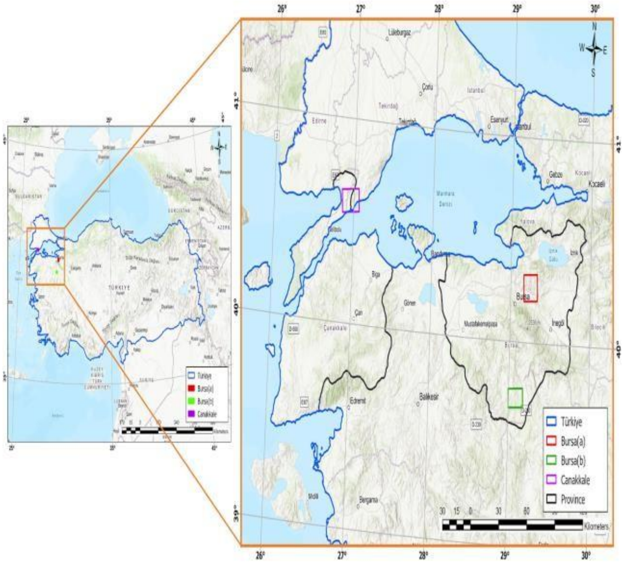

Figure 1. Study Areas

Parameter	Value Range	Default Value
Points_per_side	16–512	32
Crop_n_layers	1–10	0
Pred_iou_thresh	0.5–1	0.88
Stability_score_thresh	0.5–1	0.95
Crop_n_points downscale factor	1–5	1
Min_mask_region area	10–1000	1

Table 1. SAM configuration parameters used in this study.

For each site, pre-fire and immediate post-fire Sentinel-2 Level-2A multispectral images were acquired in order to maximize the spectral contrast between burned and unburned surfaces and to minimize the influence of post-fire vegetation recovery. All images were subjected to atmospheric correction using the standard Sen2Cor processing chain and were subsequently co-registered to a common spatial reference framework to ensure precise pixel-level alignment between multi-temporal scenes. Accurate geometric consistency between pre- and post-fire acquisitions is particularly critical for change-based indices, since even minor misalignments may introduce artificial spectral variations and boundary artifacts.

To enhance the separability of fire-affected areas, a spectrally guided three-band composite was generated by combining

ΔNBR, ΔNBR2 and ΔNDVI difference layers. This composite representation was specifically designed to amplify post-fire spectral responses related to char and ash deposition, vegetation loss and moisture changes, while suppressing background variability caused by phenological differences and illumination effects. The resulting composite image was subsequently normalized and rescaled to match the dynamic range required by the SAM input interface, which expects standard three-channel RGB imagery.

This spectrally enhanced composite served as the primary input for the zero-shot segmentation experiments. By embedding physically meaningful fire-related spectral information into an RGB-like format, the proposed preprocessing strategy enables the SAM model originally trained on natural images to better focus its mask generation mechanism on fire-disturbed surfaces. Figure 2 presents representative pre-fire and post-fire false-color Sentinel-2 images together with the derived index-based composite for the study areas.

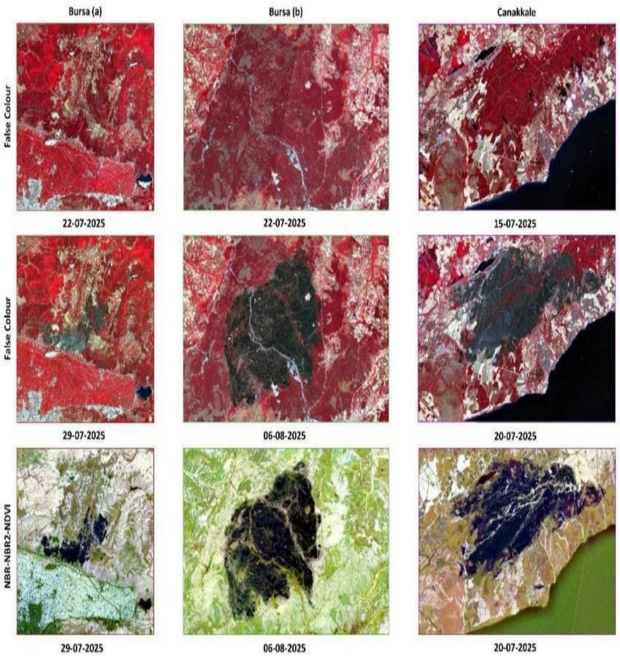

Figure 2. Pre-fire and post-fire Sentinel-2 false-color images and post-fire composite derived from ΔNBR, ΔNBR2 and ΔNDVI indices

2.2 Segment Anything Model (SAM) and Zero-Shot Configuration

The Segment Anything Model (SAM) was employed in a strictly zero-shot configuration, without any form of fine-tuning or domain-specific retraining. In order to guide the automatic mask proposal process toward regions most likely affected by fire, spatially constrained prompt points were generated within areas exhibiting high ΔNBR values. These automatically extracted point prompts were used to initialize the segmentation process and to reduce the likelihood of generating irrelevant object masks outside burned zones.

Several internal SAM parameters controlling the sampling density, mask filtering and multi-scale inference behavior were systematically explored. Among these parameters, crop_n_layers, which governs the hierarchical multi-scale image cropping strategy, was found to exert the strongest influence on the geometric completeness of burned-area objects, boundary continuity and the preservation of narrow or fragmented fire scars. Increasing the number of crop layers enables SAM to analyze the same region at different spatial contexts and resolutions, which is particularly beneficial for burned-area mapping where both large homogeneous burn scars and small isolated patches may coexist within the same scene.

In addition to crop_n_layers, parameters related to prompt density and mask quality filtering were also varied to evaluate their impact on segmentation stability and over-segmentation behavior. The complete set of SAM configuration parameters examined in this study is summarized in Table 1. All experiments were conducted using identical preprocessing and prompt-generation strategies to ensure a fair comparison between different parameter settings.

2.3 Evaluation and Hyperparameter Analysis

The segmentation outputs produced by SAM were quantitatively evaluated using manually digitized burned-area reference boundaries generated through detailed visual interpretation of post-fire Sentinel-2 imagery. Intersection over Union (IoU) and F1-score were adopted as the primary accuracy metrics to assess both area-based agreement and the balance between omission and commission errors.

Beyond global accuracy statistics, a comprehensive qualitative assessment was also conducted to examine spatial and geometric characteristics of the extracted burned-area masks. In particular, visual inspection focused on boundary sharpness, spatial continuity of burn perimeters, preservation of fine-scale and elongated burned patches, and the ability of the model to avoid artificial fragmentation along heterogeneous land-cover transitions. Special attention was given to visually complex zones, including forest–agriculture interfaces, shadow-affected slopes and mixed vegetation structures, where spectral ambiguity is typically most pronounced.

The influence of individual SAM hyperparameters especially crop_n_layers, points_per_side, pred_iou_thresh and stability_score_thresh was analyzed in terms of both quantitative performance and qualitative geometric behavior. This dual evaluation strategy enabled a more comprehensive understanding of how zero-shot configuration choices affect segmentation reliability, boundary regularity and spatial coherence. Through this systematic hyperparameter analysis, the study identifies robust operational settings for burned-area extraction and provides practical guidance for applying SAM to post-fire mapping scenarios characterized by heterogeneous landscapes and limited reference data.

3. RESULTS AND EVALUATION

The proposed zero-shot framework demonstrated high and stable segmentation performance at both test sites, confirming its capacity to generalize across ecologically and topographically distinct fire-affected landscapes. Despite being applied without any task-specific training or labeled data, the method consistently produced spatially coherent burned-area masks and preserved the geometric structure of fire perimeters.

For the Bursa study site, the framework achieved an Intersection over Union (IoU) of 0.89 and an F1-score of 0.94. Similarly, for the Çanakkale site, an IoU of 0.87 and an F1-score of 0.92 were obtained. These accuracy levels are fully comparable to those commonly reported for supervised deep learning–based burned-area segmentation models trained on post-fire satellite imagery, while completely eliminating the need for manually annotated training samples.

A clear performance gain was observed when multi-scale inference was enabled (crop_n_layers = 2). This configuration substantially improved boundary delineation and polygon continuity, particularly along irregular and fragmented fire perimeters. The multi-scale strategy allowed the model to better integrate both local texture information and broader spatial context, resulting in more complete representation of elongated burn scars and narrow fire fronts. In contrast, single-scale configurations were more prone to producing fragmented masks and minor boundary discontinuities, especially in heterogeneous land-cover settings.

From a qualitative perspective, SAM successfully captured small, spatially isolated and disconnected burned patches that are frequently omitted by conventional ΔNBR-based thresholding methods. This capability is especially important in post-fire landscapes where low- to moderate-severity burns are distributed in a patchy manner and are difficult to isolate using global spectral thresholds. Visual inspection further revealed that the proposed spectrally guided input representation helped suppress false detections over bare soil and dark non-vegetated surfaces, which are common sources of confusion in index-driven approaches.

The main sources of disagreement between the SAM-derived masks and the reference data were observed in partially burned areas and transitional vegetation zones, where mixtures of scorched vegetation, surviving canopy and exposed soil coexist within the same pixel. In such zones, spectral ambiguity remains high and even expert-driven manual delineation is subject to uncertainty. Additional minor mismatches were also identified along shadow-affected slopes and at forest–agriculture interfaces, where abrupt land-cover transitions introduce complex spatial patterns.

Overall, the results confirm that the proposed zero-shot SAM framework provides robust and transferable performance across different fire scenarios, while offering clear advantages in terms of boundary completeness, detection of fine-scale burn features and reduced fragmentation compared to classical index-based methods. Figure 3 illustrates the visual comparison between the reference burned-area boundaries and the corresponding SAM-based segmentation results.

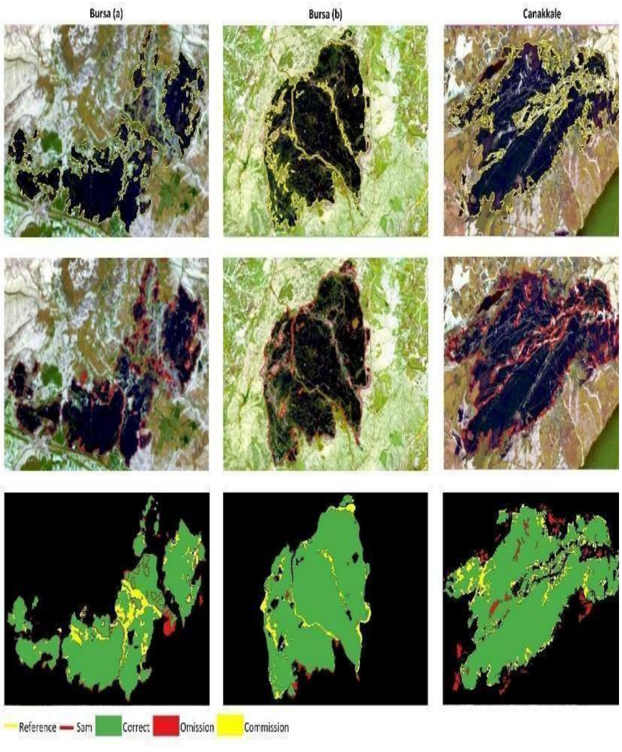

Figure 3. Comparison between reference data and SAM segmentation results

Quantitative performance analysis further confirmed that SAM configuration parameters most notably points_per_side and crop_n_layers play a decisive role in determining segmentation accuracy and computational efficiency (Figure 4). For both fire-affected landscapes in the Bursa and Çanakkale regions, the baseline configuration (points_per_side = 32, crop_n_layers = 0) produced relatively modest results, with IoU values ranging between 0.71 and 0.78. These findings indicate that single-scale sampling is insufficient to capture the complex geometric structure and heterogeneous spatial patterns of post-fire landscapes.

Increasing the sampling density by raising the points_per_side parameter from 32 to 64 led to moderate improvements in both IoU and F1 scores. However, the most substantial performance gains were obtained when the multi-scale cropping strategy was activated (crop_n_layers = 2). Under this configuration, IoU values increased to 0.83 and 0.88 for the Bursa-a and Bursa-b sub-areas, respectively, and to 0.84 for the Çanakkale site, while the corresponding F1 scores exceeded 0.90 in all cases. In particular, the highest segmentation accuracy was achieved in the Bursa-b study area, reaching an F1 score of 0.94 and an IoU of 0.89. These results clearly demonstrate that incorporating multi-scale contextual information substantially enhances boundary continuity and spatial integrity of burned-area segments.

Despite the accuracy gains obtained through denser sampling and multi-scale processing, a pronounced increase in computational cost was observed. While the (32, 2) configuration completed processing within approximately 4–6 minutes, execution time increased to 18–23 minutes for the (64, 2) configuration and escalated dramatically to 4–5 hours when an excessively dense and deep configuration such as (128, 3) was applied. Importantly, in the Bursa-a case, the (32, 2) and (64, 2) configurations produced nearly identical IoU values, yet the former completed almost forty times faster. This result highlights the practical necessity of balancing segmentation accuracy against processing time, especially in operational and large-area monitoring scenarios.

Overall, increasing points_per_side from 32 to 64 improved boundary delineation by enhancing edge sampling density, whereas the crop_n_layers = 2 setting proved critical for strengthening spatial coherence through the integration of multi-scale contextual information. Although the (64, 2) parameter combination delivered the highest overall accuracy, the (32, 2) configuration offered a highly competitive alternative with substantially lower computational demand, making it more suitable for large-scale and time-critical applications. In contrast, overly complex parameter settings, such as (128, 3), did not yield meaningful additional accuracy gains and, in several cases, increased commission errors, thereby reducing overall operational efficiency.

	points_per_side	crop_n_layers	Precision	Recall	F1	IoU	Time
Bursa(a)	32	0	0.83	0.79	0.81	0.72	38 sec
	64	0	0.82	0.82	0.82	0.77	2 min
	32	2	0.86	0.84	0.85	0.83	5 min
	64	2	0.86	0.93	0.89	0.83	20 min
	128	3	0.87	0.89	0.88	0.82	5 h 5 min
Bursa(b)	32	0	0.88	0.84	0.86	0.78	35 sec
	64	0	0.89	0.89	0.89	0.83	2 min
	32	2	0.91	0.93	0.92	0.88	4 min
	64	2	0.92	0.97	0.94	0.89	18 min
	128	3	0.93	0.93	0.93	0.89	4 h 45 min
Canakkale	32	0	0.81	0.83	0.82	0.71	39 sec
	64	0	0.82	0.84	0.83	0.77	2 min
	32	2	0.85	0.89	0.87	0.84	6 min
	64	2	0.85	0.97	0.91	0.85	23 min
	128	3	0.85	0.97	0.91	0.83	5 h 20 min

Figure 4. Accuracy evaluation metrics of burned area segmentation

In addition to the impact of SAM configuration parameters, the use of composite images derived from NBR, NBR2 and NDVI indices played a key role in supporting reliable burned-area discrimination. The combined representation effectively captured the characteristic post-fire spectral response associated with vegetation loss and shortwave infrared darkening, thereby facilitating the filtering and labeling of SAM-generated segments. Nevertheless, the most robust separation between burned and unburned surfaces was achieved when temporal change information was explicitly incorporated through the joint use of ΔNBR, ΔNBR2 and ΔNDVI layers, together with the proposed post-processing strategy. These index-based change features therefore act as a complementary component that quantitatively reinforces SAM-derived segmentation outputs, reduces spectral confusion in transitional zones, and contributes to more consistent and reliable burned-area mapping in heterogeneous landscapes.

4. CONCLUSIONS

This study presented a label-free, zero-shot burned-area mapping framework based on the Segment Anything Model (SAM) and multispectral Sentinel-2 imagery. The framework demonstrated strong segmentation performance across two ecologically distinct fire-affected landscapes in Türkiye, achieving IoU values of 0.89 and 0.87 with corresponding F1-scores of 0.94 and 0.92 for the Bursa and Çanakkale study sites, respectively, without requiring any labeled training data. These results are fully competitive with those reported for supervised deep learning approaches and confirm the operational viability of zero-shot segmentation for post-fire assessment.

Multi-scale inference with crop_n_layers = 2 was identified as the most critical configuration parameter for improving boundary completeness and spatial coherence of the extracted burned-area masks. The (32, 2) configuration offered the most favorable balance between segmentation accuracy and computational efficiency, making it particularly suitable for large-scale and time-critical operational scenarios. The spectrally guided input composite derived from ΔNBR, ΔNBR2, and ΔNDVI effectively directed SAM’s mask generation toward fire-affected regions, substantially reducing spectral confusion at burned–unburned boundaries in heterogeneous landscapes.

By eliminating the dependence on manually annotated training data, the proposed framework directly addresses the principal operational bottleneck constraining the deployment of supervised deep learning models in remote sensing practice. The findings highlight the strategic potential of large-scale foundation models as scalable, cost-effective, and transferable solutions for environmental monitoring. Future research directions include the integration of SAM-based outputs with multitemporal SAR data, the extension to global fire-monitoring applications, and the evaluation of recently released SAM variants (e.g., SAM 2) for further accuracy improvements.

ACKNOWLEDGEMENTS

This study was supported by the Scientific and Technological Research Council of Türkiye (TÜBİTAK) under grant number 2224-A.

REFERENCES

Belenguer-Plomer, M.A., Tanase, M.A., Chuvieco, E., Bovolo, F., 2021. CNN-based burned area mapping using radar and optical data. Remote Sensing of Environment, 260, 112468. https://doi.org/10.1016/j.rse.2021.112468

Bond, W.J., Keeley, J.E., 2005. Fire as a global ‘herbivore’: The ecology and evolution of flammable ecosystems. Trends in Ecology & Evolution, 20(7), 387–394. https://doi.org/10.1016/j.tree.2005.04.025

Bowman, D.M.J.S., Balch, J.K., Artaxo, P., Bond, W.J., Cochrane, M.A., D’Antonio, C.M., DeFries, R.S., Doyle, J.C., Harrison, S.P., Johnston, F.H., et al., 2009. Fire in the Earth system. Science, 324(5926), 481–484. https://doi.org/10.1126/science.1163886

Chen, L.-C., Zhu, Y., Papandreou, G., Schroff, F., Adam, H., 2018. Encoder-decoder with atrous separable convolution for semantic image segmentation. In: Proceedings of the European Conference on Computer Vision (ECCV), pp. 801–818. https://doi.org/10.1007/978-3-030-01234-2_49

Chuvieco, E., Riaño, D., Danson, F.M., Martín, P., 2006. Use of a radiative transfer model to simulate the postfire spectral response to burn severity. Journal of Geophysical Research: Biogeosciences, 111(G4). https://doi.org/10.1029/2005JG000143

Chuvieco, E., Pettinari, M.L., Lizundia-Loiola, J., Storm, T., Padilla, M., Pardo-Igúzquiza, E., 2019. Generation and analysis of a new global burned area product based on MODIS 250 m reflectance bands and thermal anomalies. Earth System Science Data, 11, 201–223. https://doi.org/10.5194/essd-11-201-2019

Drusch, M., Del Bello, U., Carlier, S., Colin, O., Fernandez, V., Gascon, F., Hoersch, B., Isola, C., Laberinti, P., Martimort, P., et al., 2012. Sentinel-2: ESA’s optical high-resolution mission for GMES operational services. Remote Sensing of Environment, 120, 25–36. https://doi.org/10.1016/j.rse.2011.11.026

Keeley, J.E., Bond, W.J., Bradstock, R.A., Pausas, J.G., Rundel, P.W., 2012. Fire in Mediterranean Ecosystems: Ecology, Evolution and Management. Cambridge University Press, Cambridge, UK.

Key, C.H., Benson, N.C., 2006. Landscape assessment: Ground measure of severity, the Composite Burn Index; and remote sensing of severity, the Normalized Burn Ratio. In: Lutes, D.C. et al. (Eds.), FIREMON: Fire Effects Monitoring and Inventory System. USDA Forest Service, pp. LA1–LA51.

Kirillov, A., Mintun, E., Ravi, N., Mao, H., Rolland, C., Gustafson, L., Xiao, T., Whitehead, S., Berg, A.C., Lo, W.-Y., et al., 2023. Segment Anything. In: Proceedings of the IEEE/CVF International Conference on Computer Vision (ICCV), pp. 4015–4026. https://doi.org/10.1109/ICCV51070.2023.00371

Lentile, L.B., Holden, Z.A., Smith, A.M.S., Falkowski, M.J., Hudak, A.T., Morgan, P., Lewis, S.A., Gessler, P.E., Benson, N.C., 2006. Remote sensing techniques to assess active fire characteristics and post-fire effects. International Journal of Wildland Fire, 15(3), 319–345. https://doi.org/10.1071/WF05097

Long, J., Shelhamer, E., Darrell, T., 2015. Fully convolutional networks for semantic segmentation. In: Proceedings of the IEEE Conference on Computer Vision and Pattern Recognition (CVPR), pp. 3431–3440. https://doi.org/10.1109/CVPR.2015.7298965

Pausas, J.G., Fernández-Muñoz, S., 2012. Fire regime changes in the Western Mediterranean Basin: From fuel-limited to drought-driven fire regime. Climatic Change, 110, 215–226. https://doi.org/10.1007/s10584-011-0060-6

Ronneberger, O., Fischer, P., Brox, T., 2015. U-Net: Convolutional networks for biomedical image segmentation. In: Proceedings of the International Conference on Medical Image Computing and Computer-Assisted Intervention (MICCAI), pp. 234–241. https://doi.org/10.1007/978-3-319-24574-4_28

Rouse, J.W., Haas, R.H., Schell, J.A., Deering, D.W., 1974. Monitoring vegetation systems in the Great Plains with ERTS. In: Proceedings of the Third Earth Resources Technology Satellite-1 Symposium, pp. 309–317.

Roy, D.P., Boschetti, L., Justice, C.O., Ju, J., 2008. The collection 5 MODIS burned area product—Global evaluation by comparison with the MODIS active fire product. Remote Sensing of Environment, 112(9), 3690–3707. https://doi.org/10.1016/j.rse.2008.05.013

Turco, M., Rosa-Cánovas, J.J., Bedia, J., Jerez, S., Montávez, J.P., Llasat, M.C., Provenzale, A., 2018. Exacerbated fires in Mediterranean Europe due to anthropogenic warming projected with nonstationary climate-fire models. Nature Communications, 9, 3821. https://doi.org/10.1038/s41467-018-06358-z

van der Werf, G.R., Randerson, J.T., Giglio, L., van Leeuwen, T.T., Chen, Y., Rogers, B.M., Mu, M., van Marle, M.J.E., Morton, D.C., Collatz, G.J., et al., 2017. Global fire emissions estimates during 1997–2016. Earth System Science Data, 9, 697–720. https://doi.org/10.5194/essd-9-697-2017

Zhu, X.X., Tuia, D., Mou, L., Xia, G.-S., Zhang, L., Xu, F., Fraundorfer, F., 2017. Deep learning in remote sensing: A comprehensive review and list of resources. IEEE Geoscience and Remote Sensing Magazine, 5(4), 8–36. https://doi.org/10.1109/MGRS.2017.2762307